

<https://helda.helsinki.fi>

---

## Omics profiling identifies the regulatory functions of the MAPK/ERK pathway in nephron progenitor metabolism

Kwon, Hyuk Nam

2022-10-01

---

Kwon , H N , Kurtzeborn , K , Iaroshenko , V , Jin , X , Loh , A , Escande-Beillard , N , Reversade , B , Park , S & Kuure , S 2022 , ' Omics profiling identifies the regulatory functions of the MAPK/ERK pathway in nephron progenitor metabolism ' , Development (Cambridge, England) , vol. 149 , no. 19 . <https://doi.org/10.1242/dev.200986>

---

<http://hdl.handle.net/10138/355227>

<https://doi.org/10.1242/dev.200986>

---

cc\_by

publishedVersion

---

*Downloaded from Helda, University of Helsinki institutional repository.*

*This is an electronic reprint of the original article.*

*This reprint may differ from the original in pagination and typographic detail.*

*Please cite the original version.*

## RESEARCH ARTICLE

# Omics profiling identifies the regulatory functions of the MAPK/ERK pathway in nephron progenitor metabolism

Hyuk Nam Kwon<sup>1,2,\*</sup>, Kristen Kurtzeborn<sup>1,2,\*</sup>, Vladislav Iaroshenko<sup>1,2</sup>, Xing Jin<sup>3</sup>, Abigail Loh<sup>4</sup>, Nathalie Escande-Beillard<sup>4,5</sup>, Bruno Reversade<sup>4,6</sup>, Sunghyok Park<sup>3</sup> and Satu Kuure<sup>1,2,7,‡</sup>

## ABSTRACT

Nephron endowment is defined by fetal kidney growth and crucially dictates renal health in adults. Defects in the molecular regulation of nephron progenitors contribute to only a fraction of reduced nephron mass cases, suggesting alternative causative mechanisms. The importance of MAPK/ERK activation in nephron progenitor maintenance has been previously demonstrated, and here, we characterized the metabolic consequences of MAPK/ERK deficiency. Liquid chromatography/mass spectrometry-based metabolomics profiling identified 42 reduced metabolites, of which 26 were supported by *in vivo* transcriptional changes in MAPK/ERK-deficient nephron progenitors. Among these, mitochondria, ribosome and amino acid metabolism, together with diminished pyruvate and proline metabolism, were the most affected pathways. *In vitro* cultures of mouse kidneys demonstrated a dosage-specific function for pyruvate in controlling the shape of the ureteric bud tip, a regulatory niche for nephron progenitors. *In vivo* disruption of proline metabolism caused premature nephron progenitor exhaustion through their accelerated differentiation in pyrroline-5-carboxylate reductases 1 (*Pycr1*) and 2 (*Pycr2*) double-knockout kidneys. *Pycr1/Pycr2*-deficient progenitors showed normal cell survival, indicating no changes in cellular stress. Our results suggest that MAPK/ERK-dependent metabolism functionally participates in nephron progenitor maintenance by monitoring pyruvate and proline biogenesis in developing kidneys.

**KEY WORDS:** Organogenesis, Tissue-specific progenitors, *Pycr1/Pycr2*, Self-renewal, Differentiation, Development, Metabolism, Receptor tyrosine kinase signaling, Intracellular signaling cascades

<sup>1</sup>Helsinki Institute of Life Science, University of Helsinki, Helsinki, FIN-00014, Finland. <sup>2</sup>Stem Cells and Metabolism Research Program, Faculty of Medicine, University of Helsinki, Helsinki, FIN-00014, Finland. <sup>3</sup>College of Pharmacy, Natural Product Research Institute, Seoul National University, Seoul 08826, Korea. <sup>4</sup>Institute of Molecular and Cellular Biology (IMCB), A\*STAR, Singapore 138648, Singapore. <sup>5</sup>Stem Cells and Metabolism Research Program, Faculty of Medicine, University of Helsinki, Helsinki, FIN-00014, Finland. <sup>6</sup>Medical Genetics Department, School of Medicine, Koç University, Istanbul 34010, Turkey. <sup>7</sup>GM-unit, Laboratory Animal Center, Helsinki Institute of Life Science, University of Helsinki, Helsinki, FIN-00014, Finland.

\*These authors contributed equally to this work

‡Author for correspondence (satu.kuure@helsinki.fi)

id V.I., 0000-0003-0046-0536; A.L., 0000-0003-0038-4510; N.E., 0000-0002-7706-1608; B.R., 0000-0002-4070-7997; S.P., 0000-0003-1981-3274; S.K., 0000-0002-9076-0622

This is an Open Access article distributed under the terms of the Creative Commons Attribution License (<https://creativecommons.org/licenses/by/4.0>), which permits unrestricted use, distribution and reproduction in any medium provided that the original work is properly attributed.

Handling Editor: Irene Miguel-Aliaga  
Received 25 May 2022; Accepted 25 August 2022

## INTRODUCTION

The differentiation capacity of embryonic nephron progenitors (NPs) is a crucial factor for lifelong renal health as the extent of fetal nephrogenesis determines an individual's final nephron number, and low nephron count predicts a higher risk of renal complications (Luyckx and Brenner, 2010; Bertram et al., 2011). Embryonic kidney development is orchestrated by intercellular and intracellular signaling taking place between two mesodermal derivatives, the ureteric bud (UB) and the metanephric mesenchyme (MM) (Davidson et al., 2019; Kurtzeborn et al., 2019). The process of UB branching both patterns and expands kidney size, whereas the MM hosts NPs, which give rise to all segments of the functional nephron (Costantini and Kopan, 2010). Together, the UB, stromal cells in the most cortical part of the developing kidney and the MM form the NP niche, in which balanced maintenance and propagation of NPs occurs (Oxburgh, 2018). The complex interplay of signals originating from all niche compartments maintains their cell identities without much time-dependent change in niche composition, but with clear differences in cell behaviors and molecular players.

The total NP lifespan is limited to the fetal period in humans and to the first postnatal days of life in mice (Hinchliffe et al., 1991; Hartman et al., 2007; Ryan et al., 2018). The molecular regulation of NP maintenance and differentiation has been extensively studied (O'Brien, 2019; Li et al., 2021a), but the factors contributing to the cessation of the nephrogenic program are only about emerging and suggest involvement of changes in signal transduction activities (Brown et al., 2015; Volovelsky et al., 2018; Li et al., 2021b). Moreover, information is only emerging about the metabolic events and especially mitochondrial metabolism underlying the cell-type-specific behaviors of NPs during their propagation and differentiation switches (Cargill and Sims-Lucas, 2018; Tortelote et al., 2021). A recent study demonstrated higher glycolysis dependence in younger versus older NPs and showed that glycolysis inhibition promotes differentiation, in line with the requirement for aerobic glycolysis (also known as the Warburg effect) in the maintenance of pluripotency (Liu et al., 2017; Shyh-Chang and Ng, 2017). Additionally, Von Hippel-Lindau (VHL) tumor suppressor (*Vhl*) appears to be important for mitochondrial respiration in NPs, which show mild differentiation deficiency in the NP-specific absence of *Vhl* (Cargill et al., 2019).

Although one of the major energy precursors for mitochondria, namely pyruvate, is essential for normal early embryonic development and is suggested to contribute to the cell-fate switches in embryonic stem cells (Conaghan et al., 1993; Butcher et al., 1998; Moussaieff et al., 2015), general understanding of its functions in organogenesis is missing. The last step of pyruvate production is regulated by the embryonic kidney-expressed glycolytic enzyme pyruvate kinase isozyme M2 (PKM2, encoded by *Pkm*); its function is controlled by mitogen-activated protein kinase/extracellular signal-

regulated kinase (MAPK/ERK) and its reduced activity has been shown to protect against kidney injury (Yang et al., 2012; Zhou et al., 2019). PKM2, similarly to MAPK/ERK activity, regulates the cell cycle in embryonic cardiomyocytes (Purcell et al., 2007; Maejima et al., 2012; Ihermann-Hella et al., 2014; Magadam et al., 2020).

We have recently demonstrated the importance of MAPK/ERK activity in the transmission of extracellular signals for NP regulation, in which it, on the one hand, maintains NP identity and, on the other hand, propels differentiation in nephron precursors (Ihermann-Hella et al., 2018; Kurtzeborn et al., 2019; Li et al., 2021a). Interestingly, the MAPK/ERK target p53 (encoded by *Trp53*) contributes to metabolic fitness in propagating NPs (Li et al., 2015). The p53 target *Rrm2b*, encoding a catalytic subunit of ribonucleotide reductase (p53R2), is required for nephron function and, interestingly, interacts with the mitochondrial proline synthesis enzymes pyrroline-5-carboxylate reductase 1 (PYCR1) and 2 (PYCR2) (Kimura et al., 2003; Powell et al., 2005; Kuo et al., 2016). Proline metabolism is heavily utilized in cancer cells and deficiencies in its metabolism are causative of many congenital disorders, including different types of cutis laxa with rare renal manifestation (Aguilera et al., 2016; de Koning, 2017; Patriarca et al., 2021). Emerging evidence also supports a regulatory role for proline in the maintenance of pluripotency at least in embryonic stem cells (D'Aniello et al., 2017; Cermola et al., 2021). Single- and double-knockout studies of *Pycr1* and *Pycr2* demonstrated the essential involvement of proline metabolism in neuronal differentiation (Escande-Beillard et al., 2020; Stum et al., 2021), but its other organ- and tissue-specific requirements remain elusive.

We used a systems biology approach to study the cellular functions that MAPK/ERK activity effectuates in NPs. Our combined RNA sequencing and metabolomics characterization of control and MAPK/ERK-deficient NPs revealed cellular metabolism as one of the most important contributing factors in NP regulation. These results establish that the MAPK/ERK pathway guides nephrogenesis in the developing kidney by regulating energy metabolism in NPs.

## RESULTS

### Transcriptional profiling reveals mitochondria and ribosomes as the cellular components most affected by loss of MAPK/ERK activation in nephron progenitors

We recently used a genetic approach to reveal the crucial function of NP-specific MAPK/ERK signaling in progenitor maintenance and propagation (Ihermann-Hella et al., 2018). NP-specific loss of MAPK/ERK activation, achieved by conditional inactivation of both *Mek* genes *Mapk2k1* and *Mapk2k2* (*Six2*-TGC<sup>tg/+</sup>; *Mek1*<sup>fl/fl</sup>; *Mek2*<sup>-/-</sup>), resulted in rapid NP deprivation due to cell-intrinsic molecular defects and changes in the niche composition. Transcriptional profiling of MAPK/ERK-deficient NPs isolated from embryonic day (E) 13.5 kidneys (before the onset of significant NP loss) identified over 5000 differentially expressed genes (DEGs) (GSE174229; Kurtzeborn et al., 2022).

An overview of the gene ontology (GO) analysis of DEGs [ $P_{\text{adj}} < 0.05$  and  $|\log_2(\text{fold change})| \geq 2$ ] in MAPK/ERK-deficient NPs using the Cytoscape plugin ClueGO (Shannon et al., 2003; Bindea et al., 2009) is listed in Table S1 and shown in Fig. 1A. This illustrates that 'oxidative phosphorylation' (18.87%) and 'ribosome biogenesis' (18.87%) are the most affected processes. Further characterization of DEGs demonstrated that genes with the GO terms 'mitochondrial inner membrane' (25.0%) and 'mitochondrion' (15.0%) together account for 40.0% of the downregulated transcripts, which is in line with our previous findings of diminished mitochondrial functions in

MAPK/ERK-deficient cells (Kurtzeborn et al., 2022). In addition to energy metabolism, ribosome-encoding transcripts represent the second largest proportion of downregulated genes in MAPK/ERK-deficient NPs (Fig. 1B).

Use of the Kyoto Encyclopedia of Genes and Genomes (KEGG) database (Ogata et al., 1999; Ashburner et al., 2000) revealed fewer pathways than Cytoscape but further strengthened ribosomal contribution, as among the most frequent GO terms were 'polysomal ribosomes', 'ribosomal subunits', 'ribosomes' and 'NADH dehydrogenase complex'. The upregulated genes were so scattered and few that their pathway analysis failed to provide a meaningful outcome.

### MAPK/ERK-deficiency diminishes the metabolism of amino acids with previous function in stem cell regulation

We next applied a liquid chromatography (LC)/mass spectrometry (MS)-based metabolomics approach to assess MAPK/ERK-affected metabolism in more detail. Reliable metabolomic analysis requires a large number of cells and this presents a challenge due to embryonic NP availability. These cells have been isolated and successfully propagated in nephrosphere cultures, but our pilot experiments revealed that using them for MAPK/ERK-regulated metabolic studies was not feasible owing to the need for extensive growth factors, additional proteins and competitive inhibitors (Brown et al., 2015; Li et al., 2016).

Guided by the results of RNA-sequencing (RNA-seq) analysis (Fig. 1), we performed targeted metabolomics analysis of the molecules involved in glycolysis and mitochondrial metabolism to quantify principally altered metabolites in an embryonic kidney mesenchyme cell line (mK4). Qualitative measurements of the LC/MS data were analyzed by partial least squares discriminant analysis (PLS-DA), a multivariate statistical technique, which showed clear discrimination for each treatment and control group in both positive and negative detection modes, while clustering well within their treatment group (Fig. 2). This revealed eight statistically different intermediate metabolites upon MAPK/ERK-deficiency induced by treatment with the MEK inhibitor U0126 (Table S2), which include components of glycolysis, the tricarboxylic acid (TCA) cycle and ATP production, supporting our and others' recent findings that the energy source is an important factor in NP regulation (Li et al., 2015; Kurtzeborn et al., 2022).

Amino acid metabolism is becoming known as an important regulator of different stem cells and their properties (Zhao et al., 2012; Kim et al., 2020; Allmeroth et al., 2021; Someya et al., 2021). To identify the wider spectrum of metabolic changes, an untargeted approach was applied to control and MEK-inhibited mK4 cells. Comparison of the untargeted tandem mass spectrometry (MS2) spectrum patterns with an online MS database revealed a significant decrease of 34 metabolites, including polyamines (N-acetylputrescine), amino acids such as glutamine and its metabolites, L-aspartic acid, leucine, proline, threonine and tryptophan (Table S2) (Melnikov et al., 2016; Krafczyk et al., 2021). Also, methionine, which was recently suggested to contribute to NP proliferation (Makayes et al., 2021), was diminished upon MAPK/ERK deficiency.

Metabolite set enrichment analysis (MSEA) of all identified metabolites by MetaboAnalyst revealed 'pentose phosphate pathway', 'Warburg effect', 'glycine/serine metabolism' and 'purine metabolism' as the most altered metabolic pathways in the absence of MAPK/ERK activation (Fig. 3A). Table S3 summarizes the results of the MSEA analysis and lists the contributing metabolites for each category. Heatmap visualization of the metabolite levels accordingly

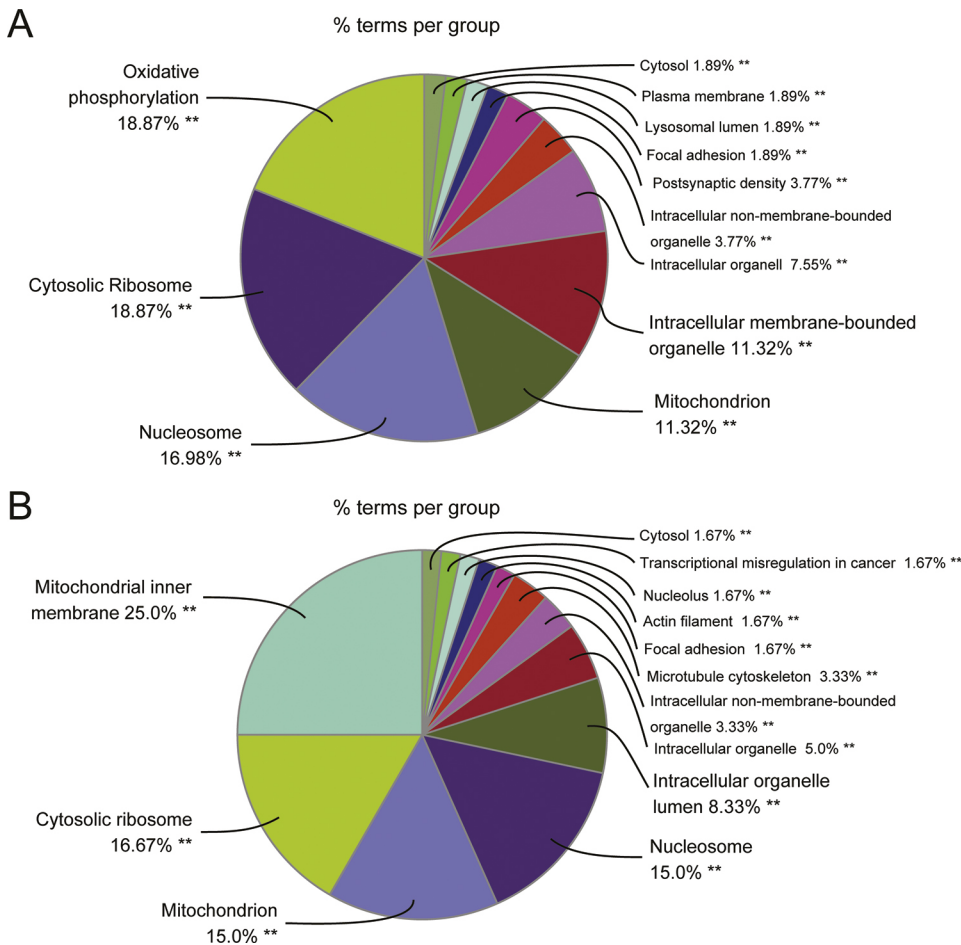


**Fig. 1. ClueGO analysis of differentially expressed transcripts in MAPK/ERK-deficient nephron progenitors.**

(A,B) Overview pie chart of cellular component and KEGG pathway analyses of the (A) total and (B) downregulated differentially expressed genes (DEGs) between control and MAPK/ERK-deficient NPs. The percentage of genes per term is shown in each group. GO analysis was performed using the Cytoscape plugin ClueGO. The pie chart shows the enriched signaling pathway categories based on the  $\kappa$  coefficient of 0.5. Significantly enriched GO terms are indicated by \*\* $P < 0.001$ .

confirmed that metabolic pathways were downregulated in MAPK/ERK-deficient cells (Fig. 3B).

### Integration of metabolomics and RNA-seq data suggests dysregulation in nephron progenitor fate decisions

To conduct a more comprehensive analysis at the systems biology level, we next integrated the information from our metabolomics and RNA-seq experiments in different metabolic pathways. The mutually

meaningful relationship between the identified LC/MS-based metabolites and RNA-seq gene expression changes was investigated by integrating the results of the two analyses, summarized in Fig. 4.

Among the 46 metabolites we identified, 28 correlated with 113 DEGs (Fig. 4; Table S4) in our RNA-seq data (GSE174229; Kurtzborn et al., 2022). Although the most significant findings underline mitochondria and energy, diminished amino acid metabolism of tryptophan, glutamine, glycine and proline are

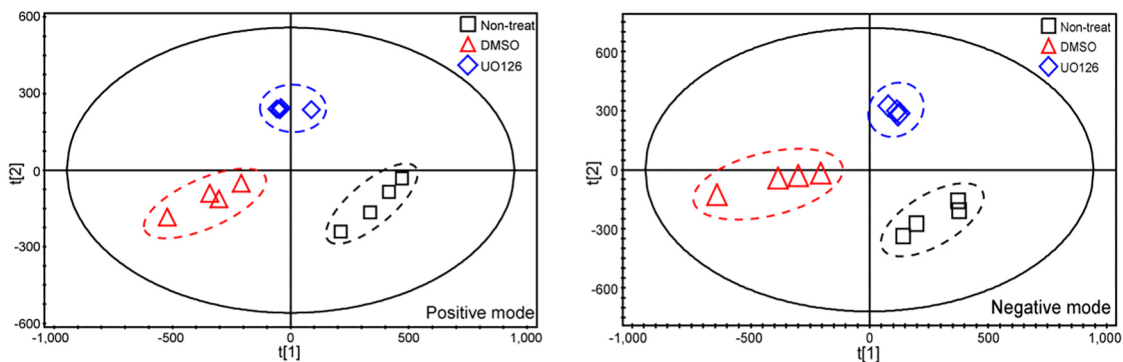


**Fig. 2. PLS-DA on LC/MS positive- and negative-mode metabolites identified in mK4 cells upon MEK inhibition.** PLS-DA score plot for mass-to-charge ratios of positive ( $R^2X=0.92$ ;  $R^2Y=0.991$ ;  $Q^2Y=0.968$ ;  $n=1+4$  components) (left) and negative ( $R^2X=0.817$ ;  $R^2Y=0.999$ ;  $Q^2Y=0.992$ ;  $n=1+1$  components) (right) detection modes for LC/MS. Each symbol represents the metabolic profile of an individual sample in each group ( $n=4$ ). Black squares indicate the non-treated group, red triangles indicate the DMSO-treated group and blue diamonds indicate the MEK inhibitor UO126-treated group. In both detection modes, MEK-inhibited cells, in which MAPK/ERK activation is abolished, share the most similar metabolic profile.  $R^2X$ , total sum of variation in X explained by the model;  $R^2Y$ , total sum of variation in Y explained by the model, representing the overall quality;  $Q^2Y$ , predictive accuracy of the model representing the overall cross-validation co-efficiency.



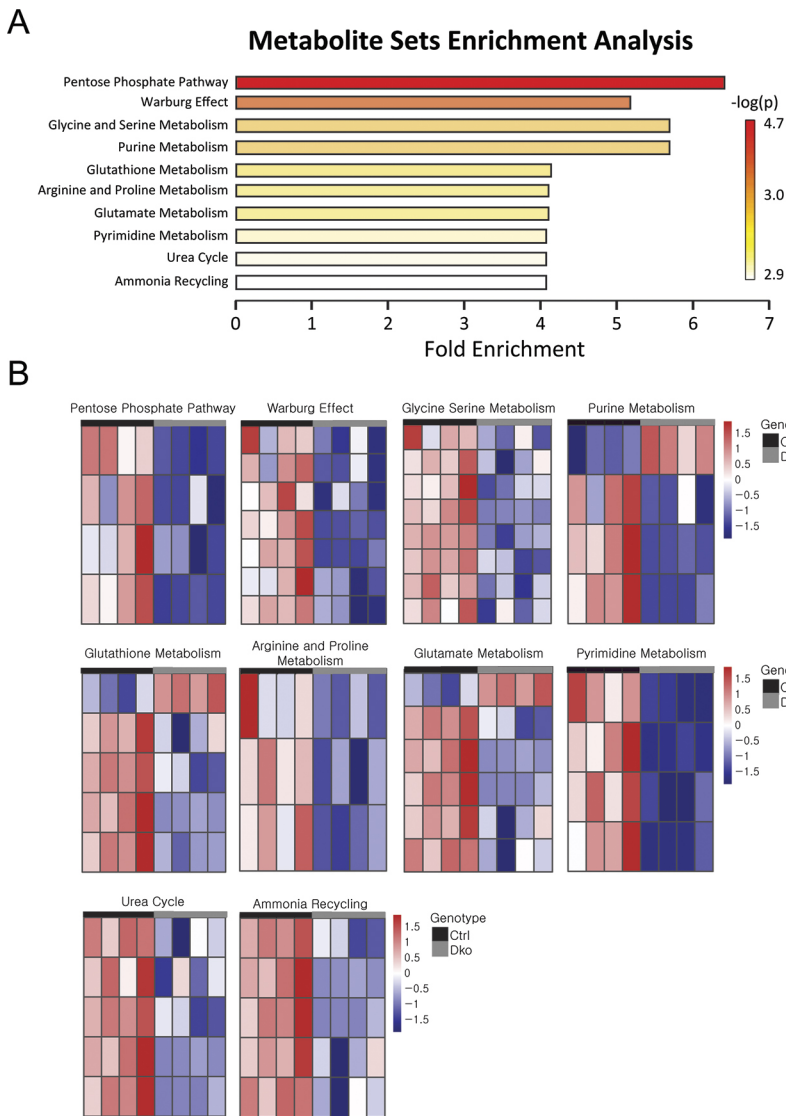


**Fig. 3. MSEA and heatmap visualization.** (A) All 46 MAPK/ERK-dependent metabolites identified by LC/MS were applied to MSEA to distinguish the most affected metabolic pathways. The horizontal bar plots are ranked by  $P$ -values. The color gradient is an indicator of how strongly a metabolic pathway changes, with the strongest changes being red and weakest changes being white. (B) Heatmap analysis of the changes in mRNA expression contributing to the differential pathways identified by MSEA. The individual differential metabolites are listed in Table S3. Each horizontal row, respectively, provides the data for the transcripts as follows: pentose phosphate pathway: D-ribose, R5P, G6P and ADP; Warburg effect: 3-PG, R5P, citrate, ADP, glutamine, G6P and glutamate; glycine serine metabolism: 3-PG, glycine, methionine, ADP, threonine, glutamate, creatine and ornithine; purine metabolism: xanthine, R5P, ADP and glutamine; glutathione metabolism: oxidized glutathione, glycine, glutamate, ADP and pyroglutamic acid; arginine and proline metabolism: N-acetyl putrescine, creatine and proline; glutamate metabolism: oxidized glutathione, glutamate, ADP, glutamine, glycine and aspartate; pyrimidine metabolism: uracil, ADP, dihydrothymine and glutamine; urea cycle: aspartate, ornithine, glutamate, ADP and glutamine; ammonia recycling: glutamate, ADP, glutamine, glycine and aspartate. Control, Ctrl; double knockout, Dko; G6P, glucose-6-phosphate; 3-PG, 3-phosphoglyceric acid; R5P, ribose-5-phosphate.

supported by *in vivo* transcriptional changes in NP cells (Fig. 4; Table S4). Of these, tryptophan has previously been shown to regulate pluripotent stem cell proliferation and expression of the pluripotency regulator *Oct4* (or *Pou5f1*); glutamine, however, regulates fate reversibility of hair follicle stem cells, and glycine being a component of glutathione functions in the antioxidant response, in one-carbon/folate metabolism with connections to the methionine cycle, and in neuronal specification (Avila et al., 2014; Cheng et al., 2015; Kim et al., 2020; Someya et al., 2021). Interestingly, proline metabolism, which not only regulates stem cell pluripotency but also contributes to the control of neuronal differentiation (Washington et al., 2010; Casalino et al., 2011; Liu et al., 2019; Escande-Beillard et al., 2020; Cermola et al., 2021; Stum et al., 2021), is downregulated in MAPK/ERK-deficient cells, and its direct regulators *Pycr2* (mitochondrial) and *Pycr1* (cytosolic) are also downregulated in MAPK/ERK-deficient NPs. The correlations of metabolite-to-gene expression changes in different pathways are visualized in Fig. 5.

The NP population is composed of cells with heterogeneous identities and stem-cell properties based on their differential expression of *Six2*, *Cited1* and *Pax2* (O'Brien, 2019). *SIX2*<sup>+</sup> NPs represent a heterogeneous population ranging from highly

undifferentiated to differentiation-committed cells (Self et al., 2006; Brunskill et al., 2014), whereas *SIX2*/*Cited1* double-positive cells represent the most stem-cell-like and, thus, undifferentiated subpopulation (Brown et al., 2013, 2015).

We next wanted to study whether one of the NP subpopulations would be more dependent on MAPK/ERK activity than the others. To do this, we compared the changes in expression in MAPK/ERK target and metabolism-related genes identified here with previously published single cell RNA-seq (scRNA-seq) results (Brunskill et al., 2014). Analysis of *p53*, a MAPK/ERK target gene present in *Six2*<sup>+</sup> cells demonstrated 100% expression in scRNA-seq datasets (Table S5). Of the metabolism-related MAPK/ERK target genes, *Pycr1* was present in 44%, *Pycr2* in 77% and *Pkm2* in 100% of the datasets. The expression of differentiation-related genes reflected the known heterogeneity of *Six2*<sup>+</sup> cells as their expression was sparser among the datasets: *Wnt4* was present in 18.75% and *Lhx1* in 12.5% of the datasets, indicating that some *Six2*<sup>+</sup> cells are committed to differentiation. This analysis demonstrates that MAPK/ERK targets have higher representation in *Six2*<sup>+</sup> cells than the differentiation markers.

As expected, *Six2*/*Cited1* double-positive cells showed reduced presence of differentiation-marker-positive datasets for *Wnt4* (16%)

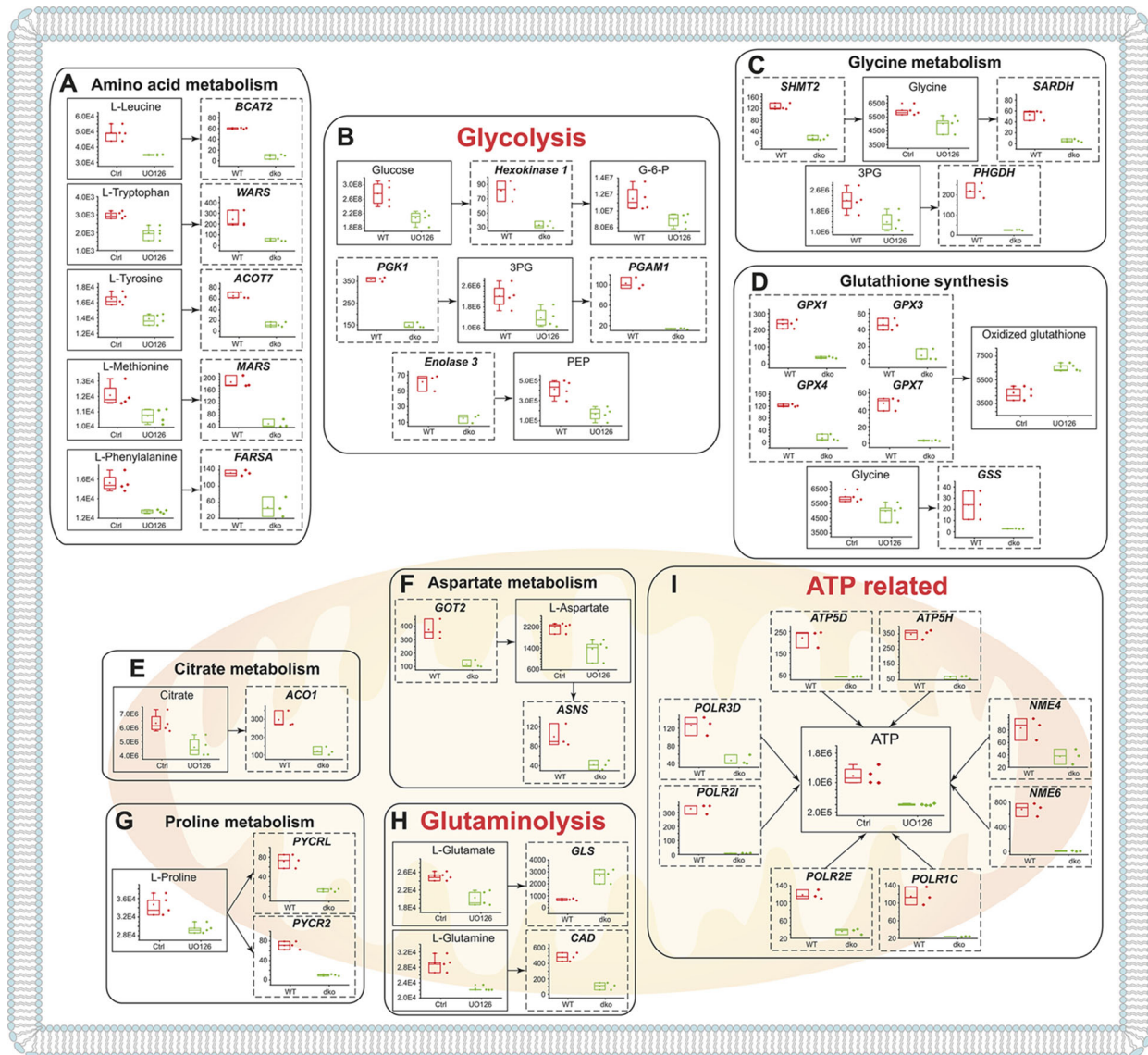


**Fig. 4. Integration of identified metabolites and transcriptional level changes of MAPK/ERK deficiency.** (A-I) Quantification of metabolite levels (shown in boxes with solid lines) and gene expression levels (shown in boxes with dashed lines) from metabolomics and RNA-seq analyses, respectively, were used to integrate transcriptional and metabolite level changes. Metabolite levels were measured by LC/MS from four independent control (DMSO-treated) and four MEK-inhibited (U0126-treated) mK4 cell samples. Gene expression level changes were retrieved from RNA-seq performed in isolated populations of three control (WT) and three *Mek1/2* double-knockout (dko) NP populations (GSE174229; Kurtzborn et al., 2022). For the box plots shown, boxes indicate the 25-75th percentiles, whiskers show the s.d., the central line indicates the average, and each dot represents an individual datapoint. Dot plots show each datapoint as distinct spots. The y-axes indicate detected metabolite levels and relative mRNA expression. (A) These analyses identified diminished levels of the amino acid L-leucine and the related mitochondrial expressed branched-chain aminotransferase 2 (*Bcat2*), which catalyzes the first reaction in the catabolism of essential branched-chain amino acids (including leucine); L-tryptophan and its producer tryptophanyl-tRNA synthetase (*Wars* or *Wars1*); L-tyrosine and acyl-CoA thioesterase 7 (*Acot7*) – acetyl-CoA derived from tyrosine via acetoacetate is catabolized by *ACOT7*; L-methionine and methionine-tRNA synthetase (*Mars* or *Mars1*); and L-phenylalanine and phenylalanyl-tRNA synthetase subunit  $\alpha$  (*Farsa*). (B) Glycolysis-related changes include those in the levels of glucose itself and the levels of the direct downstream modulators hexokinase 1 (*Hk1*) and glucose 6-phosphate (G-6-P); 3-phosphoglyceric acid (3PG) and its upstream regulator phosphoglycerate kinase 1 (*Pgk1*) and downstream metabolic modulators 3-phosphoglycerate dehydrogenase (*Phgdh*) and phosphoglycerate mutase 1 (*Pgam1*); and phosphoenolpyruvate (PEP), the levels of which depends on the activity of enolase 3 (*Eno3*), which also exhibits diminished levels. (C) Reduced glycine levels, together with reduced levels of the enzymes serine hydroxymethyltransferase 2 (*Shmt2*), which metabolizes glycine from serine, and glutathione synthetase (*Gss*) and sarcosine dehydrogenase (*Sardh*), which further metabolize glycine to glutathione and sarcosine, were seen. (D) Glutathione synthesis derives changes not only from glycine shortage (C) but also from reduced levels of glutathione peroxidases 1 (*Gpx1*), 3 (*Gpx3*), 4 (*Gpx4*) and 7 (*Gpx7*). (E) Reduced citrate metabolite levels are associated with reduced levels of aconitate hydratase 1 (*Aco1*), which balances citrate and isocitrate levels. (F) Reduced aspartate levels are associated with lower citrate levels and diminished expression of glutamic-oxaloacetic transaminase 2 (*Got2*) and asparagine synthetase (*Asns*). (G) Proline metabolism is related to both aspartate metabolism (F) and glutaminolysis (H), and reduced proline levels associate with reduced expression of proline-producing enzymes pyrroline-5-carboxylate reductase family, member 2 (*Pycr2*) and pyrroline-5-carboxylate reductase-like (*Pyr1*). (H) The levels of glutamate and glutamine metabolites together with glutamine synthetase 2 (*Gls*) and pyrimidine biosynthesis-related carbamoyl-phosphate synthetase 2 (*Cad*), are diminished. (I) Reduced ATP levels associate with several transcriptional changes in ATP synthase subunits [H<sup>+</sup> transporting, mitochondrial F1 complex,  $\delta$  subunit (*Atp5d*) and H<sup>+</sup> transporting, mitochondrial F0 complex, subunit D (*Atp5h*)], in RNA polymerase subunits [polymerase I polypeptide C (*Polr1c*), polymerase II polypeptide E (*Polr2e*), polymerase II polypeptide I (*Polr2i*) and polymerase III polypeptide D (*Polr3d*)] and in nucleoside diphosphate kinases (*Nme4* and *Nme6*).

and *Lhx1* (8%) than what was identified for *Six2*<sup>+</sup> cells (Table S5). However, the MAPK/ERK targets *p53* (100%), *Pycr1* (40%), *Pycr2* (80%) and *Pkm2* (100%) either remained highly present (*p53* and *Pkm2*) or demonstrated increased representation in the most stem-cell-like nephron progenitor population. The data together support the conclusions that MAPK/ERK functions in the maintenance of stemness and suggests that control of pyruvate and proline metabolism may participate in progenitor maintenance and propagation.

#### Only a few metabolites are increased in MAPK/ERK-deficient cells

Only four metabolites were upregulated in MAPK/ERK-deficient cells (Table S2). These included oxidized glutathione, increased levels of which associate with oxidative stress (Rossi et al., 2006; Tchanchou et al., 2021). Analysis of *in vivo* transcriptional changes in oxidative-stress-related gene signatures revealed downregulation of four major antioxidant enzymes of the glutathione peroxidase family (*Gpx1*, *Gpx3*, *Gpx4* and *Gpx7*), in conjunction with Cu/Zn superoxide dismutase (*Sod1*) and forkhead box 4 (*Foxo4*), encoding a transcription factor regulating reactive oxygen species (Table S6). Additionally, the genes encoding peroxisome biogenesis proteins (*Pex6*, *Pex16* and *Pex10*) and mitochondrial damage responders (*Pink1* and *Atf4*) were downregulated (Table S6) providing a possible link to cellular stress (Schrader and Fahimi, 2006). Interestingly, Parkin (*Prkn*), shown to be transcriptionally activated upon cellular stress (Bouman et al., 2011), was upregulated, along with a modest increase in several other oxidative stress responders including hypoxia-inducible factor 1- $\alpha$  (*Hif1a*) (Table S3). These results suggest a perturbed antioxidant defense, which may contribute to the diminished cell cycle progression, which we previously reported in MAPK/ERK-deficient NPs that do not yet show increased apoptosis (Ihermann-Hella et al., 2018).

#### Pyruvate affects nephron progenitor niche morphology in a dose-dependent manner

To investigate the physiological consequences of the identified metabolic changes, we first assayed the effect of pyruvate on early kidney development. E11.5 kidneys were cultured for 72 h *in vitro* as described earlier (Ihermann-Hella and Kuure, 2019) under normal (1 mM) and different pyruvate concentration conditions. Cultured kidneys were immunostained for calbindin to visualize ureteric bud tips, which form an extrinsic niche for NPs (O'Brien, 2019) and branching morphogenesis (Fig. 6A). Without pyruvate, kidney growth through branching morphogenesis was severely compromised (50–80% less tips), the trunks were abnormally long, and the tips failed to enlarge, especially with less than 0.5 mM pyruvate concentrations. We and others have previously published the effect of MEK inhibitor(s) on ureteric bud branching morphogenesis (Fisher et al., 2001; Hida et al., 2002; Ihermann-Hella et al., 2014). Moreover, our ureteric bud-specific genetic experiments demonstrate a very similar phenotype to that observed with chemical MEK inhibition (Ihermann-Hella et al., 2014). In essence, MAPK/ERK-deficient ureteric buds fail to generate complex branched epithelial structures. This is due to failure of ureteric bud tips, which contain the collecting duct progenitors, to expand and form an enlarged ampulla preceding the tip bifurcation required for new branch formation. The MAPK/ERK-deficient morphology resembles the ureteric bud morphology observed here in low pyruvate concentrations (Fig. 6A), thus supporting our findings that MAPK/ERK regulates progenitors by contributing to

their metabolic control. Interestingly, pyruvate concentration higher than 1 mM resulted in diminished branching and tip amounts but with a different pattern than in low concentrations (0–0.5 mM) and without a dramatic effect on tip morphology, further confirming the role of metabolism in the regulation of kidney progenitors.

#### Proline metabolism is required for nephron progenitor maintenance

Our integrated metabolomics and transcriptomics data revealed downregulation of proline metabolism, which is of particular interest as, in addition to reduction of the metabolite itself, the expression of its regulatory genes *Pycr2* and *Pycr1* was significantly diminished in MAPK/ERK-deficient NPs (Fig. 4).

The publicly available GUDMAP database (<https://www.gudmap.org/>) shows high *Pycr1* expression in the developing kidney from E11.5 onwards. Based on microarray analysis, *Pycr1* expression is highest in the NP cells and in their early differentiating descendants. The Genepaint database reveals a more restricted expression pattern for *Pycr2*, which, however, seems to overlap with *Pycr1* in differentiating nephron precursors (<https://gp3.mpg.de/viewer/setInfo/EH1140/10>). To assess the physiological *in vivo* requirement of proline metabolism in kidney development, we utilized the conventional inactivation of *Pycr1* and *Pycr2* genes in mouse. Inactivation of both *Pycr* genes resulted in Mendelian ratios of homozygous single knockouts of *Pycr1*<sup>-/-</sup> and *Pycr2*<sup>-/-</sup> as well as double-knockout *Pycr1*<sup>-/-</sup>;*Pycr2*<sup>-/-</sup> pups. Characterization of *Pycr1*<sup>-/-</sup>;*Pycr2*<sup>-/-</sup> mouse kidneys at postnatal day (P) 1 revealed no abnormalities in size and morphology based on histological examination (Fig. S1A–C).

We next analyzed the NP population and nephron differentiation in *Pycr1/Pycr2* (hereafter *Pycr1/2*) double-knockout kidneys. Visualization of PAX2-positive cells, which represent the ureteric bud, NPs and nephron precursors of the developing kidney (Naiman et al., 2017; Grimley and Dressler, 2018), suggested defective NP maintenance in the *Pycr1*<sup>-/-</sup>;*Pycr2*<sup>-/-</sup> postnatal kidneys (Fig. 6B). SIX2 expression, however, has been shown to be high in the NPs throughout fetal development but, before the final loss of NPs in postnatal wild-type (WT) kidneys at P3, it shifts to localize more abundantly in nephron precursors (Kobayashi et al., 2008; Rumballe et al., 2011). Markedly reduced numbers of SIX2-positive NP cells were detected per ureteric bud in *Pycr1*<sup>-/-</sup>;*Pycr2*<sup>-/-</sup> postnatal kidneys than in control kidneys (Fig. 6B,C), demonstrating NP cell dependence on proline metabolism.

To gain mechanistic understanding for premature NP decrease in *Pycr1*<sup>-/-</sup>;*Pycr2*<sup>-/-</sup> kidneys, we hypothesized the involvement of three contributing mechanisms: increased proliferation, decreased apoptosis or accelerated differentiation. The possible involvement of proliferation and/or apoptosis was analyzed by visualizing mitotic cells with phospho-histone H3 and apoptotic cells with cleaved-caspase 3, and these analyses showed no differences between control and *Pycr1*<sup>-/-</sup>;*Pycr2*<sup>-/-</sup> kidneys (Fig. 7G and Fig. S1D–G). Analysis of mitochondrial morphology revealed no alterations in NPs of *Pycr1*<sup>-/-</sup>;*Pycr2*<sup>-/-</sup> kidneys (Fig. S2).

We then performed immunofluorescent staining for cadherin 6 (CDH6), a nephron differentiation marker, to visualize the bulk of differentiating nephrons ranging from early pretubular aggregates to late S-shaped bodies, followed by a quantitative analysis, which demonstrated an increase in nephron precursors (Fig. 7A,B,E). We next used another differentiation commitment marker, cyclin D1 (CD1, encoded by *Ccnd1*), which detects renal vesicles that represent a more restricted precursor pool with a more defined and







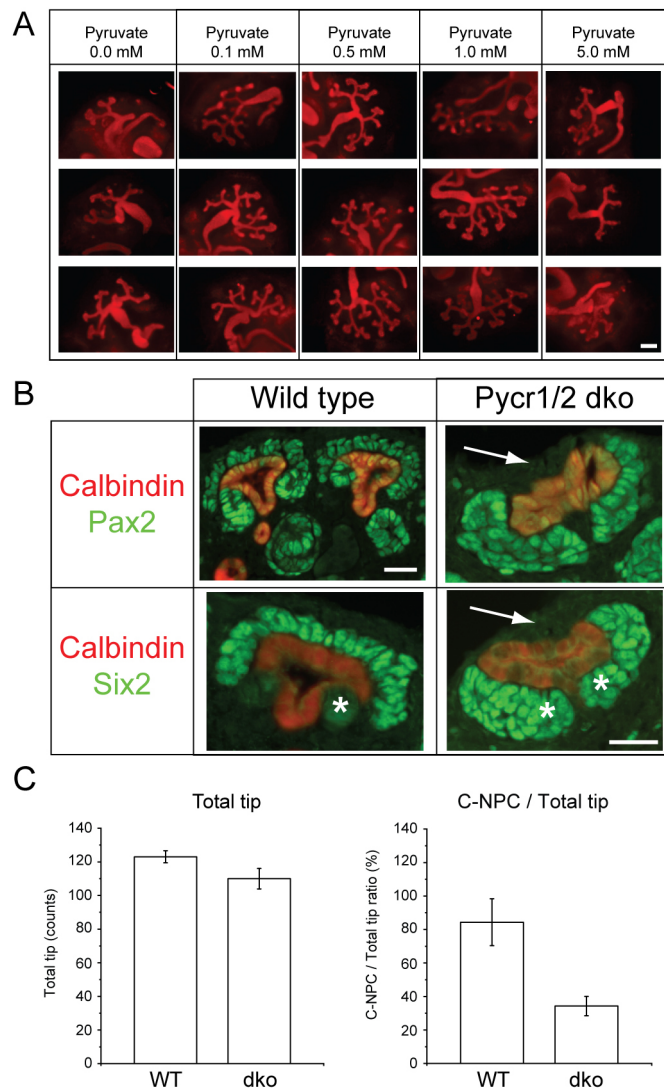


**Fig. 6. Functional characterization of identified metabolite effects on nephron progenitor biology.** (A) Embryonic kidneys at E11.5 were cultured for 72 h under different concentrations of pyruvate supplementation and immunostained for calbindin (red) to visualize the entire ureteric bud epithelium. Normal kidney culture medium contained 1 mM pyruvate, which served as a control for other concentrations. Scale bar: 200  $\mu$ m. (B) P1 control (wild-type) and *Pycr1/2* double-knockout (dko) kidneys were immunostained for PAX2 (green, marker of nephron progenitors and precursors) or SIX2 (green, marker of nephron progenitors) in combination with calbindin (red, marker of ureteric bud epithelium). White arrows indicate the regions where PAX2- and SIX2-positive NP cells should be located but were significantly diminished in the absence of *Pycr1/2*. White asterisks point to the differentiating nephron precursors, which show only very weak SIX2 signal in control kidneys, but to which SIX2 localizes almost exclusively in *Pycr1/2* double-knockout kidneys. Scale bars: 50  $\mu$ m (calbindin and Pax2 wild type); 200  $\mu$ m (calbindin and Six2 *Pycr1/2* double-knockout; also applies to calbindin and Pax2 *Pycr1/2* double-knockout and to calbindin and Six2 wild type). (C) Quantification of ureteric tip numbers (total tip) and cortical nephron progenitor cells (C-NPCs) per each tip in the cortex of control and *Pycr1/2* double-knockout kidneys ( $n=2$  kidneys/genotype, a total of 15 randomly selected medullar sections were counted). Data are average $\pm$ s.d.

proline metabolism, which, in this study, was identified to depend on MAPK/ERK activation, is essential for preventing premature differentiation of the postnatal NPs, through which it contributes to progenitor maintenance.

## DISCUSSION

Systems biology is emerging as a powerful approach to study functional linkages of metabolic and transcriptional changes (Kitano, 2002; Pang et al., 2019). Metabolomics has the potential to link genotype to phenotype (Fiehn, 2002), and it has been broadly and successfully used in systems biology studies (Weckwerth, 2003) to gain a better understanding of complex biological systems, as exemplified by metabolomics studies of mitochondrial dysfunction in kidney diseases (Nam et al., 2009; McKillop and Flatt, 2011; Atzler et al., 2014; Sharma et al., 2013; Tran et al., 2016). We have previously demonstrated the importance of the MAPK/ERK pathway in NP maintenance and differentiation during embryonic kidney development (Ihmann-Hella et al., 2018). Here, we combine metabolomics and transcriptomics characterization of MAPK/ERK-deficient NP cells to advance the understanding of cellular mechanisms contributing to kidney development.

Congenital anomalies of the kidney and urinary tract (CAKUT) are common birth defects caused by abnormalities in kidney morphogenesis and contribute to the worldwide burden of kidney diseases (Anand et al., 2014; Luyckx et al., 2018; Jain and Chen, 2019). The CAKUT phenotype spectrum varies from mild renal hypoplasia with reduced nephron count to hypodysplasia and a complete lack of kidneys (Murugapooopathy and Gupta, 2020). The milder CAKUT forms, such as reduced nephron mass due to impaired NP maintenance or differentiation, are not life-threatening at early ages but increase the risk of chronic kidney disease with cardiovascular comorbidities later in life (Luyckx and Brenner, 2010; Bertram et al., 2011). As the final nephron count in each individual is determined by renal morphogenesis during fetal development, any factor possibly affecting the rate and extent of nephrogenesis is of high interest.

Our results indicate that MAPK/ERK-deficiency affects both pyruvate and proline metabolism, which are interconnected through glycolysis and glutaminolysis (Fig. 5). Pyruvate, an end product of glycolysis, is converted into acetyl coenzyme A (acetyl-CoA) to feed the mitochondrial TCA cycle. Proline is mainly synthesized from glutamate during glutaminolysis (De Ingeniis et al., 2012), which has crucial compensatory functions under glucose-deprivation conditions owing to its ability to convert glutamine into glutamate (Wu et al., 2014; Yang et al., 2014). As glycolysis and glutaminolysis are the main energy metabolism pathways in mammals, they both likely contribute to energy deprivation in MAPK/ERK-deficient cells.

The production of pyruvate requires the function of the embryonic kidney-expressed and MAPK/ERK-regulated glycolytic enzyme PKM2 (Gupta and Bamezai, 2010; Yang et al., 2012). Our results demonstrated decreased expression of *Pkm2* and reduced levels of the TCA intermediate citrate in MAPK/ERK-deficient cells. Effects of different pyruvate dosages showed dose-dependent changes in the morphology of ureteric bud tips, which serve as an extrinsic niche for NPs (O'Brien, 2019). This suggests that low pyruvate availability, for example, due to diminished conversion of precursor phosphoenolpyruvate to pyruvate, supports ureteric bud growth and elongation, but fails to generate new tip niches, which are essential for NP maintenance (Li et al., 2021b). High pyruvate concentrations reduced the number of tip niches as well but without significant effects on tip morphology. Interestingly, forced redirection of pyruvate to mitochondrial acetyl-CoA production increases pluripotency, whereas glycolytic acetyl-CoA production drives histone acetylation in embryonic stem cells (Moussaieff et al., 2015), supporting a crucial role for pyruvate availability in NP stemness regulation.

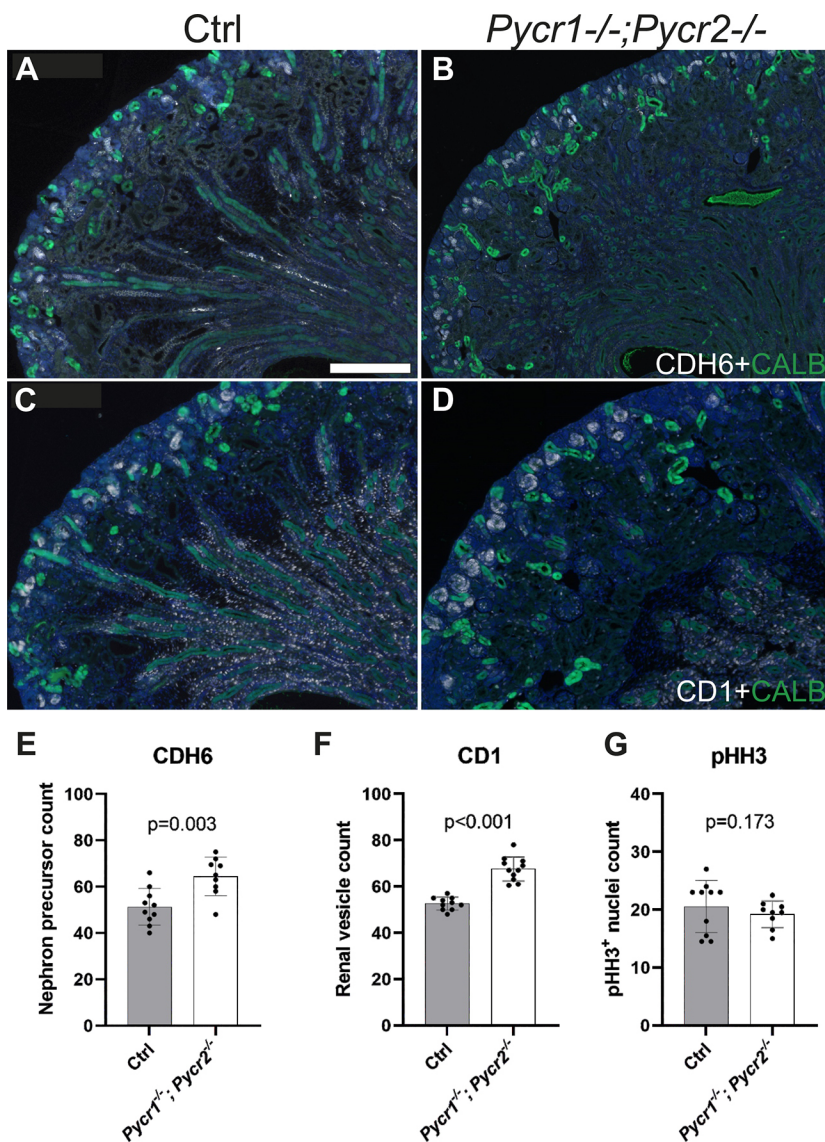


**Fig. 7. Nephron progenitors are prematurely lost in the postnatal kidneys of *Pycr1/2* double-knockout mice.** (A,B) Representative images of P1 (A) control and (B) *Pycr1/2* double-knockout kidneys, which were co-immunostained with cadherin 6 (CDH6, white) to visualize epithelializing nephrons from early pretubular aggregates to S-shaped bodies, and calbindin (CALB, green), highlighting the ureteric bud epithelium. (C,D) Representative images of immunostaining in P1 (C) control and (D) *Pycr1/2* double-knockout kidneys in which cyclin D1 (CD1, white) staining indicates differentiation-committed nephron progenitors in the renal vesicles and calbindin (CALB, green) highlights the ureteric bud epithelium. Scale bar: 200  $\mu$ m. (E-G) Quantification of (E) cadherin 6-positive and (F) cyclin D1-positive differentiating nephrons as well as (G) overall proliferation [phospho-histone H3 (pHH3) was used as a mitotic marker] in control and *Pycr1/2* dko kidneys ( $n=3$  kidneys/genotype, 3-5 randomly selected medullar sections were counted). Data are average  $\pm$  s.d. A Mann-Whitney test was used to determine significance.

Proline metabolism has versatile functions in cellular homeostasis (Patriarca et al., 2021) and its role as a stem-cell regulator is of high relevance to our study. Proline supplementation to embryonic stem cells induces their proliferation and induction towards epiblast fate, whereas maternal proline improves nutrient transport to better support pre-implantation embryo development (Washington et al., 2010; Casalino et al., 2011; Cermola et al., 2021; Someya et al., 2021). Proline deficiency causes several different inherited diseases that typically affect growth, the central nervous system, and renal functions (Patriarca et al., 2021).

Our *in vivo* characterization of *Pycr1/2*-deficient kidneys revealed the importance of proline metabolism for NP maintenance in the postnatal kidney. Our results show that in the developing kidney, *Pycr2* can compensate the loss of *Pycr1*, in accordance with the recent report on their genetic interactions (Stum et al., 2021). Interestingly, although PYCR1-deficiency, which in humans causes cutis laxa, causes cell death in the mouse central nervous system and in *Xenopus* and zebrafish skin (Reversade et al., 2009; Kuo et al., 2016; Escande-Beillard et al., 2020), *Pycr1/2*-deficient kidneys did not show increased apoptosis. Instead, the loss of the enzymes involved in the last steps of proline biosynthesis induced premature differentiation in NPs of the postnatal kidneys.

Identification of proline as one of the regulators of NP cells is an important result, not only because the exact functions of proline metabolism at the organ and tissue levels have remained unknown, but also owing to its therapeutic potential as a metabolite that is easy to administer.

It has been shown that under pyruvate deprivation, glutaminolysis increases the concentration of mitochondrial glutamate, which can be converted into pyrroline 5-carboxylate (P5C), an intermediate metabolic product that contributes to both the biosynthesis and catabolism of proline. As proline is mainly synthesized from glutamate or ornithine (Jones, 1985), decreased levels of mitochondrial glutamate due to poorly functioning glutaminolysis may directly affect P5C production and contribute to defective proline synthesis in MAPK/ERK-deficient cells (Fig. 5).

In this study, we focused on understanding MAPK/ERK-dependent transcriptional and metabolic control of NP cell maintenance, propagation and differentiation. For this, NP cells with intact and depleted MAPK/ERK activity were used. This strategy is a powerful way to study NP niche-intrinsic mechanisms of nephrogenesis guidance. However, it bypasses the biological complexity of whole-kidney morphogenesis, which depends on the



functions of the ureteric bud epithelium and stroma. We and others have shown that several ureteric bud-derived signals significantly contribute to NP cell biology (Karner et al., 2011; Lindström et al., 2015; Li et al., 2021b) and the regulatory function of stromal signals is emerging (Naiman et al., 2017; Zhang et al., 2019). Thus, further studies are needed to build up a holistic view of how NP metabolism is integrated in the control of an optimally functioning kidney.

## MATERIALS AND METHODS

### RNA isolation for sequencing and data analysis

For sequencing, RNA was isolated from nephron progenitors sorted by fluorescence-activated cell sorting at E13.5 using a standard protocol for chloroform/isopropanol extraction, followed by DNase I treatment according to the manufacturer's instructions (Thermo Fisher Scientific, EN0521). Total RNA quantity and quality were estimated using the Bioanalyzer RNA Total Pico (Agilent Technologies) and NanoDrop spectrophotometer analysis. Library preparation was done using NuGen Ovation Solo (<https://lifesciences.tecan.com/ovation-solo-rna-seq-library-preparation-nuquant?p=tab-1>) and sequencing was performed with NextSeq 500 (Illumina) at the BIDGEN DNA Sequencing and Genomics Laboratory (University of Helsinki). To convert BCL files to FASTQ files and demultiplex samples, bcl2fastq2 Conversion Software was used (Illumina). Sequenced reads were trimmed for adaptor sequence and masked for low-complexity or low-quality sequences using Trimmomatic (Illumina). Trimmed reads were mapped to the GENCODE *Mus musculus* release M23 reference genome GRCm38 using STAR aligner (2.6.0c) ([https://www.gencodegenes.org/mouse/release\\_M23.html](https://www.gencodegenes.org/mouse/release_M23.html)).

Raw gene counts were normalized using the DESeq2 R package (v.3.6.2) and sample clustering was visualized by principal component analysis. Multiple testing adjustment of *P*-values was done using the Benjamini–Hochberg method to compare gene expression levels in three control and three nephron-specific MAPK/ERK-deficient samples (*Six2-TGC*, *Mek1<sup>fl/fl</sup>* and *Mek2<sup>-/-</sup>*). The RNA-seq raw data is available at GEO (GSE174229; Kurtzeborn et al., 2022).

### Gene Ontology and pathway analysis

To analyze the differing metabolic characteristics of MAPK/ERK-deficient NP populations, we used our recent whole-genome RNA-seq data (GSE174229; Kurtzeborn et al., 2022). To interpret DEGs in NPs, we performed pathway analysis using the Cytoscape plugin ClueGO (<https://apps.cytoscape.org/apps/cluego>) to create a functionally organized gene ontology. The GO Cellular Component and KEGG ontology were used for GO analyses, and we performed the GO analyses using total DEGs and upregulated and downregulated DEGs separately.

### Sample preparation for metabolomics

To investigate metabolic changes in NPs caused by MEK inhibition, we analyzed metabolic changes in the mK4 cell line, derived from embryonic kidney mesenchyme, through a LC/MS-based metabolomics approach. Prior to cell harvesting for metabolite extraction, mK4 cells were incubated with dimethyl sulfoxide (DMSO, 0.1% v/v) or MEK inhibitor U0126 (15  $\mu$ M, Sigma Aldrich, 9903), or cultured without treatment. After 24 h incubation, cells were harvested using 0.25% trypsin/EDTA (Gibco, 25200056) treatment and washed with ice-cold PBS. The metabolites were extracted using the methods described in Kurtzeborn et al. (2022). In brief, harvested cells were dissolved in 600  $\mu$ l of methanol/chloroform solvent (2:1 v/v), flash frozen twice with liquid nitrogen and thawed at room temperature. Then, 200  $\mu$ l chloroform and 200  $\mu$ l distilled water were sequentially added, and metabolites were separated by centrifugation at 15,000 *g* for 20 min at 4°C. Finally, water-soluble metabolites (upper phase after centrifugation) were dried using a centrifugal vacuum evaporator. The protein aggregate (middle phase) was isolated and dissolved in 6 M urea buffer, and total protein concentration was measured for normalization.

### LC/MS analysis

Chromatographic separation was performed on a ZIC-HILIC column (3.5  $\mu$ m, 200 Å, 100×2.1 mm; Merck Millipore) using an Acquity UPLC system (Waters, MA, USA). The column temperature was 35°C with a flow rate of 0.4 ml/min and the auto-sampler cooler temperature was 4°C with an injection volume of 2  $\mu$ l. Analytes were eluted with a mobile phase composed of 10 mM ammonium acetate in water with pH 6.8 (buffer A) and 10 mM ammonium acetate in water:acetonitrile solution (1:3) with pH 6.8 (buffer B). The gradient conditions were as follows: 0–1 min, 100% buffer B; 1–7 min, decreasing concentration of buffer B from 100% to 20%; 7–11 min, 20% buffer B; 11–23 min 100% buffer B. MS experiments were performed on a Q Exactive Focus Orbitrap Mass Spectrometer (Thermo Fisher Scientific) equipped with heated electrospray ionization sources. To detect as many ions as possible, both positive and negative detection modes were used in the LC/MS experiment. The inclusion list for parallel reaction methods is shown in Table S7. The MS2 spectrum patterns were compared with the online MS database (Wishart et al., 2018). The METLIN database and high-resolution *m/z* from the full MS experiment were applied to confirm target metabolites (Guijas et al., 2018). All the measured data were normalized against total protein concentration.

### Metabolomics analysis and systems biology

Multivariate statistical analysis was carried out using SIMCA-P (Umetrics, Umeå, Sweden; v. 11.0). To distinguish metabolic pattern differences from each experimental group, the supervised statistical method PLS-DA was performed using the processed data from LC/MS positive and negative modes, and the metabolites contributing to separation on PLS-DA were identified. To further analyze the identified metabolites, we carried out MSEA using a web-based tool from MetaboAnalyst (Xia and Wishart, 2010), and the levels of individual contributing metabolites from the MSEA results were visualized by heatmap analysis in R.

### Mouse lines

*Six2-TGC*, *Mek1<sup>fl/fl</sup>* and *Mek2<sup>-/-</sup>* mice and their genotyping have been described previously (Scholl et al., 2007; Kobayashi et al., 2008; Belanger et al., 2003). Mice were kept in mixed genetic backgrounds containing C57BL6/Rcc and 129/SvEv strains. The kidneys were dissected at indicated stages according to a published protocol (Ihmann-Hella and Kuure, 2019). Animal husbandry and procedures were approved by EU legislation and the Finnish Animal Care and Use Committee.

### Effect of pyruvate on embryonic kidney culture

E11.5 wild-type mouse kidneys were cultured under different concentrations of pyruvate supplementation for 72 h in Dulbecco's Modified Eagle Medium (Gibco, 41965-039) supplemented with 10% fetal bovine serum (ThermoFisher, 10500064), GlutaMAX (Sigma Aldrich, 35350038) and antibiotics. Cultured embryonic kidneys were analyzed by immunostaining for calbindin (1:500, Santa Cruz Biotechnology, sc-7691), which labels the ureteric bud epithelium, allowing us to examine the effect of pyruvate concentration on ureteric bud branching.

### Hematoxylin-Eosin staining, immunofluorescence detection of nephron progenitors and precursors, imaging and quantification

P1 kidneys from *Pycr1/2* mating were collected and fixed with 4% paraformaldehyde, after which they were processed with paraffin and sectioned according to standard procedures. Hematoxylin-Eosin and immunofluorescence staining, and imaging procedures were performed as previously described (Conaghan et al., 1993). The following primary antibodies were used: anti-cadherin 6 (1:400, a gift from Greg Dressler, University of Michigan, Ann Arbor, MI, USA), anti-calbindin (1:500, Santa Cruz Biotechnology, sc-7691), anti-cleaved caspase 3 (1:200, Cell Signaling Technologies, 9664), anti-cyclin D1 (1:400, PharMingen, 14726E, lot 7823-04), anti-phospho-histone H3 (1:500, Cell Signaling Technologies, 9706), anti-PAX2 (1:400, Invitrogen, 71-6000), anti-TOM20 (1:300, Santa Cruz Biotechnology, sc-19554) and anti-SIX2 (1:500, ProteinTech, 11562-1-AP). Alexa Fluor-conjugated secondary antibodies (1:400; Jackson ImmunoResearch) were used. Images were acquired using a Zeiss AxioImager wide-field microscope with 40× objective and and



scanned with a Pannoramic 250 Flash II with 20× objective. Quantification of nephron progenitor cells, ureteric tips and T-buds was performed blindly by three independent researchers each counting 15 medullary sections in two wild-type and two double-knockout *Pycr1/2* kidneys. The means of the three counts were used to calculate the number of cortical nephron progenitors per each ureteric tip.

#### Acknowledgements

We thank Dr Tom Barnsby (Biomedicum Stem Cell Center, Faculty of Medicine, University of Helsinki, Finland) for discussions and comments on our manuscript. This work was carried out with help from the following institutional core facilities that are part of the Biocenter Finland infrastructures: Biomedicum Imaging Unit, Biomedicum Flow Cytometry, DNA Sequencing and Genomics, GM-unit, and Laboratory Animal Centre.

#### Competing interests

The authors declare no competing or financial interests.

#### Author contributions

Conceptualization: S.K.; Methodology: H.N.K., K.K., V.I., X.J., S.P., S.K.; Validation: H.N.K., S.K.; Formal analysis: H.N.K.; Investigation: H.N.K., K.K., V.I., S.K.; Resources: K.K., X.J., A.L., N.E.-B., B.R., S.P., S.K.; Data curation: H.N.K., K.K., V.I.; Writing - original draft: H.N.K., K.K., S.K.; Writing - review & editing: H.N.K., K.K., N.E.-B., B.R., S.K.; Visualization: H.N.K., K.K., S.K.; Supervision: B.R., S.P., S.K.; Project administration: S.K.; Funding acquisition: S.K.

#### Funding

This work was supported by funds from the Academy of Finland (309997 to S.K.), the Finnish Cultural Foundation (Suomen Kulttuurirahasto; to S.K. and H.N.K.), the Maud Kuistila Foundation (Maud Kuistilan Muistosäätiö; to S.K. and K.K.), Pediatric Cancer Foundation Väre (Lasten Syöpäsäätiö Värein; to S.K.), Aamu Pediatric Cancer Foundation (S.K.) and the Orion Research Foundation (Orionin Tutkimussäätiö; K.K.). Open Access funding provided by the Aamu Pediatric Cancer Foundation. Deposited in PMC for immediate release.

#### Peer review history

The peer review history is available online at <https://journals.biologists.com/dev/lookup/doi/10.1242/dev.200986.reviewer-comments.pdf>.

#### References

- Aguilera, O., Munoz-Sagastibelza, M., Torrejon, B., Borrero-Palacios, A., Del Puerto-Navado, L., Martinez-Useros, J., Rodriguez-Remirez, M., Zazo, S., Garcia, E., Fraga, M. et al. (2016). Vitamin C uncouples the Warburg metabolic switch in KRAS mutant colon cancer. *Oncotarget* **7**, 47954-47965. doi:10.18632/oncotarget.10087
- Allmeroth, K., Kim, C. S., Annibal, A., Pouikli, A., Koester, J., Derisbourg, M. J., Andrés Chacón-Martínez, C., Latza, C., Antebi, A. and Tessarz, P. (2021). N 1-acetylspermidine is a determinant of hair follicle stem cell fate. *J. Cell Sci.* **134**, jcs252767. doi:10.1242/jcs.252767
- Anand, S., Khanam, M. A. and Finkelstein, F. O. (2014). Global perspective of kidney disease. In *Nutrition in Kidney Disease* (L. Byham-Gray, J. Burrowes, G. Chertow, eds), pp. 11-23. Springer. doi:10.1007/978-1-62703-685-6\_2
- Ashburner, M., Ball, C. A., Blake, J. A., Botstein, D., Butler, H., Cherry, J. M., Davis, A. P., Dolinski, K., Dwight, S. S. and Eppig, J. T. (2000). Gene ontology: tool for the unification of biology. *Nat. Genet.* **25**, 25-29. doi:10.1038/75556
- Atzler, D., Schwedhelm, E. and Zeller, T. (2014). Integrated genomics and metabolomics in nephrology. *Nephrol. Dial. Transplant.* **29**, 1467-1474. doi:10.1093/ndt/gft492
- Avila, A., Vidal, P. M., Tielens, S., Morelli, G., Laguesse, S., Harvey, R. J., Rigo, J.-M. and Nguyen, L. (2014). Glycine receptors control the generation of projection neurons in the developing cerebral cortex. *Cell Death Differ.* **21**, 1696-1708. doi:10.1038/cdd.2014.75
- Belanger, L. F., Roy, S., Tremblay, M., Brott, B., Steff, A. M., Mourad, W., Hugo, P., Erikson, R. and Charon, J. (2003). Mek2 is dispensable for mouse growth and development. *Mol. Cell Biol.* **23**, 4778-4787. doi:10.1128/MCB.23.14.4778-4787.2003
- Bertram, J. F., Douglas-Denton, R. N., Diouf, B., Hughson, M. D. and Hoy, W. E. (2011). Human nephron number: implications for health and disease. *Pediatr. Nephrol.* **26**, 1529-1533. doi:10.1007/s00467-011-1843-8
- Bindea, G., Mlecnik, B., Hackl, H., Charoentong, P., Tosolini, M., Kirilovsky, A., Fridman, W.-H., Pagès, F., Trajanoski, Z. and Galon, J. (2009). ClueGO: a cytoscape plug-in to decipher functionally grouped gene ontology and pathway annotation networks. *Bioinformatics* **25**, 1091-1093. doi:10.1093/bioinformatics/btp101
- Bouman, L., Schlierf, A., Lutz, A. K., Shan, J., Deinlein, A., Kast, J., Galehdar, Z., Palmisano, V., Patenge, N., Berg, D. et al. (2011). Parkin is transcriptionally regulated by ATF4: evidence for an interconnection between mitochondrial stress and ER stress. *Cell Death Differ.* **18**, 769-782. doi:10.1038/cdd.2010.142
- Brown, A. C., Muthukrishnan, S. D., Guay, J. A., Adams, D. C., Schafer, D. A., Fetting, J. L. and Oxburgh, L. (2013). Role for compartmentalization in nephron progenitor differentiation. *Proc. Natl. Acad. Sci. USA* **110**, 4640-4645. doi:10.1073/pnas.1213971110
- Brown, A. C., Muthukrishnan, S. D. and Oxburgh, L. (2015). A synthetic niche for nephron progenitor cells. *Dev. Cell* **34**, 229-241. doi:10.1016/j.devcel.2015.06.021
- Brunskill, E. W., Park, J. S., Chung, E., Chen, F., Magella, B. and Potter, S. S. (2014). Single cell dissection of early kidney development: multilineage priming. *Development* **141**, 3093-3101. doi:10.1242/dev.110601
- Butcher, L., Coates, A., Martin, K. L., Rutherford, A. J. and Leese, H. J. (1998). Metabolism of pyruvate by the early human embryo. *Biol. Reprod.* **58**, 1054-1056. doi:10.1095/biolreprod58.4.1054
- Cargill, K. and Sims-Lucas, S. (2018). Metabolic requirements of the nephron. *Pediatr. Nephrol.* **35**, 1-8. doi:10.1007/s00467-018-4157-2
- Cargill, K., Hemker, S. L., Clugston, A., Murali, A., Mukherjee, E., Liu, J., Bushnell, D., Bodnar, A. J., Saifudeen, Z., Ho, J. et al. (2019). Von Hippel-Lindau acts as a metabolic switch controlling nephron progenitor differentiation. *J. Am. Soc. Nephrol.* **30**, 1192-1205. doi:10.1681/ASN.2018111170
- Casalino, L., Comes, S., Lambazzi, G., De Stefano, B., Filosa, S., De Falco, S., De Cesare, D., Minchiotti, G. and Patriarca, E. J. (2011). Control of embryonic stem cell metastability by L-proline catabolism. *J. Mol. Cell Biol.* **3**, 108-122. doi:10.1093/jmcb/mjr001
- Cermola, F., D'Aniello, C., Tatè, R., De Cesare, D., Martinez-Arias, A., Minchiotti, G. and Patriarca, E. J. (2021). Gastruloid development competence discriminates different states of pluripotency. *Stem Cell Rep.* **16**, 354-369. doi:10.1016/j.stemcr.2020.12.013
- Cheng, J., Li, W., Kang, B., Zhou, Y., Song, J., Dan, S., Yang, Y., Zhang, X., Li, J., Yin, S. et al. (2015). Tryptophan derivatives regulate the transcription of Oct4 in stem-like cancer cells. *Nat. Commun.* **6**, 7209. doi:10.1038/ncomms8209
- Conaghan, J., Handyside, A. H., Winston, R. M. and Leese, H. J. (1993). Effects of pyruvate and glucose on the development of human preimplantation embryos in vitro. *J. Reprod. Fertil.* **99**, 87-95. doi:10.1530/jrf.0.0990087
- Costantini, F. and Kopan, R. (2010). Patterning a complex organ: branching morphogenesis and nephron segmentation in kidney development. *Dev. Cell* **18**, 698-712. doi:10.1016/j.devcel.2010.04.008
- D'Aniello, C., Habibi, E., Cermola, F., Paris, D., Russo, F., Fiorenzano, A., Di Napoli, G., Melick, D. J., Cobellis, G., Angelini, C. et al. (2017). Vitamin C and L-proline antagonistic effects capture alternative states in the pluripotency continuum. *Stem Cell Rep.* **8**, 1-10. doi:10.1016/j.stemcr.2016.11.011
- Davidson, A. J., Lewis, P., Przepiorski, A. and Sander, V. (2019). Turning mesoderm into kidney. *Semin. Cell Dev. Biol.* **91**, 86-93. doi:10.1016/j.semcdb.2018.08.016
- De Ingeniis, J., Ratnikov, B., Richardson, A. D., Scott, D. A., Aza-Blanc, P., De, S. K., Kazanov, M., Pellicchia, M., Ronai, Z., Osterman, A. L. et al. (2012). Functional specialization in proline biosynthesis of melanoma. *PLoS One* **7**, e45190. doi:10.1371/journal.pone.0045190
- de Koning, T. J. (2017). Amino acid synthesis deficiencies. *J. Inher. Metab. Dis.* **40**, 609-620. doi:10.1007/s10545-017-0063-1
- Escande-Beillard, N., Loh, A., Saleem, S. N., Kanata, K., Hashimoto, Y., Altunoglu, U., Metoska, A., Grandjean, J., Ng, F. M., Pomp, O. et al. (2020). Loss of PYCR2 causes neurodegeneration by increasing cerebral glycine levels via SHMT2. *Neuron* **107**, 82-94.e6. doi:10.1016/j.neuron.2020.03.028
- Fiehn, O. (2002). Metabolomics—the link between genotypes and phenotypes. *Plant Mol. Biol.* **48**, 155-171. doi:10.1023/A:1013713905833
- Fisher, C. E., Michael, L., Barnett, M. W. and Davies, J. A. (2001). Erk MAP kinase regulates branching morphogenesis in the developing mouse kidney. *Development* **128**, 4329-4338. doi:10.1242/dev.128.21.4329
- Grimley, E. and Dressler, G. R. (2018). Are Pax proteins potential therapeutic targets in kidney disease and cancer? *Kidney Int.* **94**, 259-267. doi:10.1016/j.kint.2018.01.025
- Guijas, C., Montenegro-Burke, J. R., Domingo-Almenara, X., Palermo, A., Warth, B., Hermann, G., Koellensperger, G., Huan, T., Uritboonthai, W., Aisporna, A. E. et al. (2018). METLIN: a technology platform for identifying knowns and unknowns. *Anal. Chem.* **90**, 3156-3164. doi:10.1021/acs.analchem.7b04424
- Gupta, V. and Bamezai, R. N. (2010). Human pyruvate kinase M2: a multifunctional protein. *Protein Sci.* **19**, 2031-2044. doi:10.1002/pro.505
- Hartman, H. A., Lai, H. L. and Patterson, L. T. (2007). Cessation of renal morphogenesis in mice. *Dev. Biol.* **310**, 379-387. doi:10.1016/j.ydbio.2007.08.021
- Hida, M., Omori, S. and Awazu, M. (2002). ERK and p38 MAP kinase are required for rat renal development. *Kidney Int.* **61**, 1252-1262. doi:10.1046/j.1523-1755.2002.00273.x
- Hinchliffe, S. A., Sargent, P. H., Howard, C. V., Chan, Y. F. and van Velzen, D. (1991). Human intrauterine renal growth expressed in absolute number of

- glomeruli assessed by the disector method and Cavalieri principle. *Lab. Invest.* **64**, 777-784.
- Ihermann-Hella, A. and Kuure, S. (2019). Mouse ex vivo kidney culture methods. *Methods Mol. Biol.* **1926**, 23-30. doi:10.1007/978-1-4939-9021-4\_2
- Ihermann-Hella, A., Lume, M., Miinalainen, I. J., Pirttiniemi, A., Gui, Y., Peränen, J., Charron, J., Saarna, M., Costantini, F. and Kuure, S. (2014). Mitogen-activated protein kinase (MAPK) pathway regulates branching by remodeling epithelial cell adhesion. *PLoS Genet.* **10**, e1004193. doi:10.1371/journal.pgen.1004193
- Ihermann-Hella, A., Hirashima, T., Kupari, J., Kurtzborn, K., Li, H., Kwon, H. N., Cebrian, C., Soofi, A., Dapkunas, A., Miinalainen, I. et al. (2018). Dynamic MAPK/ERK activity sustains nephron progenitors through niche regulation and primes precursors for differentiation. *Stem Cell Rep.* **11**, 912-928. doi:10.1016/j.stemcr.2018.08.012
- Jain, S. and Chen, F. (2019). Developmental pathology of congenital kidney and urinary tract anomalies. *Clin. Kidney J.* **12**, 382-399. doi:10.1093/ckj/sfy112
- Jones, M. E. (1985). Conversion of glutamate to ornithine and proline: pyrroline-5-carboxylate, a possible modulator of arginine requirements. *J. Nutr.* **115**, 509-515. doi:10.1093/jn/115.4.509
- Karner, C. M., Das, A., Ma, Z., Self, M., Chen, C., Lum, L., Oliver, G. and Carroll, T. J. (2011). Canonical Wnt9b signaling balances progenitor cell expansion and differentiation during kidney development. *Development* **138**, 1247-1257. doi:10.1242/dev.057646
- Kim, C. S., Ding, X., Allmeroth, K., Biggs, L. C., Kolenc, O. I., L'Hoest, N., Chacon-Martinez, C. A., Edlich-Muth, C., Giavalisco, P., Quinn, K. P. et al. (2020). Glutamine metabolism controls stem cell fate reversibility and long-term maintenance in the hair follicle. *Cell Metab.* **32**, 629-642.e8. doi:10.1016/j.cmet.2020.08.011
- Kimura, T., Takeda, S., Sagiya, Y., Gotoh, M., Nakamura, Y. and Arakawa, H. (2003). Impaired function of p53R2 in Rrm2b-null mice causes severe renal failure through attenuation of dNTP pools. *Nat. Genet.* **34**, 440-445. doi:10.1038/ng1212
- Kitano, H. (2002). Systems biology: a brief overview. *Science* **295**, 1662-1664. doi:10.1126/science.1069492
- Kobayashi, A., Valerius, M. T., Mugford, J. W., Carroll, T. J., Self, M., Oliver, G. and McMahon, A. P. (2008). Six2 defines and regulates a multipotent self-renewing nephron progenitor population throughout mammalian kidney development. *Cell Stem Cell* **3**, 169-181. doi:10.1016/j.stem.2008.05.020
- Krafczyk, R., Qi, F., Sieber, A., Mehler, J., Jung, K., Frishman, D. and Lassak, J. (2021). Proline codon pair selection determines ribosome pausing strength and translation efficiency in bacteria. *Commun. Biol.* **4**, 589. doi:10.1038/s42003-021-02115-z
- Kuo, M. L., Lee, M. B., Tang, M., den Besten, W., Hu, S., Sweredoski, M. J., Hess, S., Chou, C. M., Changou, C. A., Su, M. et al. (2016). PYCR1 and PYCR2 interact and collaborate with RRM2B to protect cells from overt oxidative stress. *Sci. Rep.* **6**, 18846. doi:10.1038/srep18846
- Kurtzborn, K., Kwon, H. N. and Kuure, S. (2019). MAPK/ERK signaling in regulation of renal differentiation. *Int. J. Mol. Sci.* **20**, 1779. doi:10.3390/ijms20071779
- Kurtzborn, K., Kwon, H. N., Iaroshenko, V., Faisal, I., Ambroz, M., Jin, X., Qureshi, T., Kupari, J., Ihermann-Hella, A., Vaananen, J. et al. (2022). Comparative whole-genome transcriptome analysis in renal cell populations reveals high tissue specificity of MAPK/ERK targets in embryonic kidney. *BMC Biol.* **20**, 112. doi:10.1186/s12915-022-01309-z
- Li, Y., Liu, J., Li, W., Brown, A., Baddoo, M., Li, M., Carroll, T., Oxburgh, L., Feng, Y. and Saifudeen, Z. (2015). p53 Enables metabolic fitness and self-renewal of nephron progenitor cells. *Development* **142**, 1228-1241. doi:10.1242/dev.111617
- Li, Z., Araoka, T., Wu, J., Liao, H. K., Li, M., Lazo, M., Zhou, B., Sui, Y., Wu, M. Z., Tamura, I. et al. (2016). 3D culture supports long-term expansion of mouse and human nephrogenic progenitors. *Cell Stem Cell* **19**, 516-529. doi:10.1016/j.stem.2016.07.016
- Li, H., Hohenstein, P. and Kuure, S. (2021a). Embryonic kidney development, stem cells and the origin of Wilms tumor. *Genes* **12**, 318. doi:10.3390/genes12020318
- Li, H., Kurtzborn, K., Kupari, J., Gui, Y., Siefker, E., Lu, B., Matlik, K., Olfat, S., Montano-Rodriguez, A. R., Huh, S. H. et al. (2021b). Postnatal prolongation of mammalian nephrogenesis by excess fetal GDNF. *Development* **148**, dev197475. doi:10.1242/dev.197475
- Lindström, N. O., Carragher, N. O. and Hohenstein, P. (2015). The PI3K pathway balances self-renewal and differentiation of nephron progenitor cells through  $\beta$ -catenin signaling. *Stem Cell Rep.* **4**, 551-560. doi:10.1016/j.stemcr.2015.01.021
- Liu, J., Edgington-Giordano, F., Dugas, C., Abrams, A., Katakam, P., Satou, R. and Saifudeen, Z. (2017). Regulation of nephron progenitor cell self-renewal by intermediary metabolism. *J. Am. Soc. Nephrol.* **28**, 3323-3335. doi:10.1681/ASN.2016111246
- Liu, N., Dai, Z., Zhang, Y., Chen, J., Yang, Y., Wu, G., Tso, P. and Wu, Z. (2019). Maternal L-proline supplementation enhances fetal survival, placental development, and nutrient transport in mice. *Biol. Reprod.* **100**, 1073-1081. doi:10.1093/biolre/foy240
- Luyckx, V. A. and Brenner, B. M. (2010). The clinical importance of nephron mass. *J. Am. Soc. Nephrol.* **21**, 898-910. doi:10.1681/ASN.2009121248
- Luyckx, V. A., Tonelli, M. and Stanifer, J. W. (2018). The global burden of kidney disease and the sustainable development goals. *Bull. W.H.O.* **96**, 414. doi:10.2471/BLT.17.206441
- Maejima, Y., Galeotti, J., Molkenin, J. D., Sadoshima, J. and Zhai, P. (2012). Constitutively active MEK1 rescues cardiac dysfunction caused by overexpressed GSK-3 $\alpha$  during aging and hemodynamic pressure overload. *Am. J. Physiol. Heart Circ. Physiol.* **303**, H979-H988. doi:10.1152/ajpheart.00415.2012
- Magadum, A., Singh, N., Kurian, A. A., Munir, I., Mehmood, T., Brown, K., Sharkar, M. T. K., Chepurko, E., Sassi, Y., Oh, J. G. et al. (2020). Pkm2 regulates cardiomyocyte cell cycle and promotes cardiac regeneration. *Circulation* **141**, 1249-1265. doi:10.1161/CIRCULATIONAHA.119.043067
- Makayes, Y., Resnick, E., Hinden, L., Aizenshtein, E., Shlomi, T., Kopan, R., Nechama, M. and Volovelsky, O. (2021). Increasing mTORC1 pathway activity or methionine supplementation during pregnancy reverses the negative effect of maternal malnutrition on the developing kidney. *J. Am. Soc. Nephrol.* **32**, 1898-1912. doi:10.1681/ASN.2020091321
- McKillop, A. M. and Flatt, P. R. (2011). Emerging applications of metabolomic and genomic profiling in diabetic clinical medicine. *Diabetes Care* **34**, 2624-2630. doi:10.2337/dc11-0837
- Melnikov, S., Mailliot, J., Rigger, L., Neuner, S., Shin, B. S., Yusupova, G., Dever, T. E., Micura, R. and Yusupov, M. (2016). Molecular insights into protein synthesis with proline residues. *EMBO Rep.* **17**, 1776-1784. doi:10.15252/embr.201642943
- Moussaieff, A., Rouleau, M., Kitsberg, D., Cohen, M., Levy, G., Barasch, D., Nemirovski, A., Shen-Orr, S., Laevsky, I., Amit, M. et al. (2015). Glycolysis-mediated changes in acetyl-CoA and histone acetylation control the early differentiation of embryonic stem cells. *Cell Metab.* **21**, 392-402. doi:10.1016/j.cmet.2015.02.002
- Murugapopathy, V. and Gupta, I. R. (2020). A primer on congenital anomalies of the kidneys and urinary tracts (CAKUT). *Clin. J. Am. Soc. Nephrol.* **15**, 723-731. doi:10.2215/CJN.12581019
- Naiman, N., Fujioka, K., Fujino, M., Valerius, M. T., Potter, S. S., McMahon, A. P. and Kobayashi, A. (2017). Repression of interstitial identity in nephron progenitor cells by Pax2 establishes the nephron-interstitium boundary during kidney development. *Dev. Cell* **41**, 349-365.e3. doi:10.1016/j.devcel.2017.04.022
- Nam, H., Chung, B. C., Kim, Y., Lee, K. and Lee, D. (2009). Combining tissue transcriptomics and urine metabolomics for breast cancer biomarker identification. *Bioinformatics* **25**, 3151-3157. doi:10.1093/bioinformatics/btp558
- O'Brien, L. L. (2019). Nephron progenitor cell commitment: striking the right balance. *Semin. Cell Dev. Biol.* **91**, 94-103. doi:10.1016/j.semcdb.2018.07.017
- Ogata, H., Goto, S., Sato, K., Fujibuchi, W., Bono, H. and Kanehisa, M. (1999). KEGG: Kyoto Encyclopedia of genes and genomes. *Nucleic Acids Res.* **27**, 29-34. doi:10.1093/nar/27.1.29
- Oxburgh, L. (2018). Kidney nephron determination. *Annu. Rev. Cell Dev. Biol.* **34**, 427-450. doi:10.1146/annurev-cellbio-100616-060647
- Pang, H., Jia, W. and Hu, Z. (2019). Emerging applications of metabolomics in clinical pharmacology. *Clin. Pharmacol. Ther.* **106**, 544-556. doi:10.1002/cpt.1538
- Patriarca, E. J., Cermola, F., D'Aniello, C., Fico, A., Guardiola, O., De Cesare, D. and Minchiotti, G. (2021). The multifaceted roles of proline in cell behavior. *Front. Cell Dev. Biol.* **9**, 728576. doi:10.3389/fcell.2021.728576
- Powell, D. R., Desai, U., Sparks, M. J., Hansen, G., Gay, J., Schrick, J., Shi, Z. Z., Hicks, J. and Vogel, P. (2005). Rapid development of glomerular injury and renal failure in mice lacking p53R2. *Pediatr. Nephrol.* **20**, 432-440. doi:10.1007/s00467-004-1696-5
- Purcell, N. H., Wilkins, B. J., York, A., Saba-El-Leil, M. K., Meloche, S., Robbins, J. and Molkenin, J. D. (2007). Genetic inhibition of cardiac ERK1/2 promotes stress-induced apoptosis and heart failure but has no effect on hypertrophy in vivo. *Proc. Natl. Acad. Sci. USA* **104**, 14074-14079. doi:10.1073/pnas.0610906104
- Reversade, B., Escande-Beillard, N., Dimopoulou, A., Fischer, B., Chng, S. C., Li, Y., Shboul, M., Tham, P. Y., Kayserlii, H., Al-Gazali, L. et al. (2009). Mutations in PYCR1 cause cutis laxa with progeroid features. *Nat. Genet.* **41**, 1016-1021. doi:10.1038/ng.413
- Rossi, R., Dalle-Donne, I., Milzani, A. and Giustarini, D. (2006). Oxidized forms of glutathione in peripheral blood as biomarkers of oxidative stress. *Clin. Chem.* **52**, 1406-1414. doi:10.1373/clinchem.2006.067793
- Rumballe, B. A., Georgas, K. M., Combes, A. N., Ju, A. L., Gilbert, T. and Little, M. H. (2011). Nephron formation adopts a novel spatial topology at cessation of nephrogenesis. *Dev. Biol.* **360**, 110-122. doi:10.1016/j.ydbio.2011.09.011
- Ryan, D., Sutherland, M. R., Flores, T. J., Kent, A. L., Dahlstrom, J. E., Puelles, V. G., Bertram, J. F., McMahon, A. P., Little, M. H., Moore, L. et al. (2018). Development of the human fetal kidney from mid to late gestation in male and female infants. *EBioMedicine* **27**, 275-283. doi:10.1016/j.ebiom.2017.12.016
- Scholl, F. A., Dumesic, P. A., Barragan, D. I., Harada, K., Bissonauth, V., Charron, J. and Khavari, P. A. (2007). Mek1/2 MAPK kinases are essential for Mammalian development, homeostasis, and Raf-induced hyperplasia. *Dev. Cell* **12**, 615-629. doi:10.1016/j.devcel.2007.03.009

- Schrader, M. and Fahimi, H. D. (2006). Peroxisomes and oxidative stress. *Biochim. Biophys. Acta* **1763**, 1755-1766. doi:10.1016/j.bbamcr.2006.09.006
- Self, M., Lagutin, O. V., Bowling, B., Hendrix, J., Cai, Y., Dressler, G. R. and Oliver, G. (2006). Six2 is required for suppression of nephrogenesis and progenitor renewal in the developing kidney. *EMBO J.* **25**, 5214-5228. doi:10.1038/sj.emboj.7601381
- Shannon, P., Markiel, A., Ozier, O., Baliga, N. S., Wang, J. T., Ramage, D., Amin, N., Schwikowski, B. and Ideker, T. (2003). Cytoscape: a software environment for integrated models of biomolecular interaction networks. *Genome Res.* **13**, 2498-2504. doi:10.1101/gr.1239303
- Sharma, K., Karl, B., Mathew, A. V., Gangotri, J. A., Wassel, C. L., Saito, R., Pu, M., Sharma, S., You, Y. H., Wang, L. et al. (2013). Metabolomics reveals signature of mitochondrial dysfunction in diabetic kidney disease. *J. Am. Soc. Nephrol.* **24**, 1901-1912. doi:10.1681/ASN.2013020126
- Shyh-Chang, N. and Ng, H. H. (2017). The metabolic programming of stem cells. *Genes Dev.* **31**, 336-346. doi:10.1101/gad.293167.116
- Someya, S., Tohyama, S., Kameda, K., Tanosaki, S., Morita, Y., Sasaki, K., Kang, M. I., Kishino, Y., Okada, M., Tani, H. et al. (2021). Tryptophan metabolism regulates proliferative capacity of human pluripotent stem cells. *iScience* **24**, 102090. doi:10.1016/j.isci.2021.102090
- Stum, M. G., Tadenev, A. L. D., Seburn, K. L., Miers, K. E., Poon, P. P., McMaster, C. R., Robinson, C., Kane, C., Silva, K. A., Cliften, P. F. et al. (2021). Genetic analysis of Pycr1 and Pycr2 in mice. *Genetics* **218**, iyab048.
- Tchantchou, F., Miller, C., Goodfellow, M., Puche, A. and Fiskum, G. (2021). Hypobaric-induced oxidative stress facilitates homocysteine transsulfuration and promotes glutathione oxidation in rats with mild traumatic brain injury. *J. Cent. Nerv. Syst. Dis.* **13**, 1179573520988193. doi:10.1177/1179573520988193
- Tortelote, G. G., Colón-Leyva, M. and Saifudeen, Z. (2021). Metabolic programming of nephron progenitor cell fate. *Pediatr. Nephrol.* **36**, 2155-2164. doi:10.1007/s00467-020-04752-8
- Tran, M. T., Zsengeller, Z. K., Berg, A. H., Khankin, E. V., Bhasin, M. K., Kim, W., Clish, C. B., Stillman, I. E., Karumanchi, S. A., Rhee, E. P. et al. (2016). PGC1 $\alpha$  drives NAD biosynthesis linking oxidative metabolism to renal protection. *Nature* **531**, 528-532. doi:10.1038/nature17184
- Volovelsky, O., Nguyen, T., Jarmas, A. E., Combes, A. N., Wilson, S. B., Little, M. H., Witte, D. P., Brunskill, E. W. and Kopan, R. (2018). Hamartin regulates cessation of mouse nephrogenesis independently of Mtor. *Proc. Natl. Acad. Sci. USA* **115**, 5998-6003. doi:10.1073/pnas.1712955115
- Washington, J. M., Rathjen, J., Felquer, F., Lonic, A., Bettess, M. D., Hamra, N., Semendric, L., Tan, B. S., Lake, J. A., Keough, R. A. et al. (2010). L-Proline induces differentiation of ES cells: a novel role for an amino acid in the regulation of pluripotent cells in culture. *Am. J. Physiol. Cell Physiol.* **298**, C982-C992. doi:10.1152/ajpcell.00498.2009
- Weckwerth, W. (2003). Metabolomics in systems biology. *Annu. Rev. Plant Biol.* **54**, 669-689. doi:10.1146/annurev.arplant.54.031902.135014
- Wishart, D. S., Feunang, Y. D., Marcu, A., Guo, A. C., Liang, K., Vazquez-Fresno, R., Sajed, T., Johnson, D., Li, C., Karu, N. et al. (2018). HMDB 4.0: the human metabolome database for 2018. *Nucleic Acids Res.* **46**, D608-D617. doi:10.1093/nar/gkx1089
- Wu, H., Li, Z., Yang, P., Zhang, L., Fan, Y. and Li, Z. (2014). PKM2 depletion induces the compensation of glutaminolysis through  $\beta$ -catenin/c-Myc pathway in tumor cells. *Cell. Signal.* **26**, 2397-2405. doi:10.1016/j.cellsig.2014.07.024
- Xia, J. and Wishart, D. S. (2010). MSEA: a web-based tool to identify biologically meaningful patterns in quantitative metabolomic data. *Nucleic Acids Res.* **38**, W71-W77. doi:10.1093/nar/gkq329
- Yang, W., Zheng, Y., Xia, Y., Ji, H., Chen, X., Guo, F., Lyssiotis, C. A., Aldape, K., Cantley, L. C. and Lu, Z. (2012). ERK1/2-dependent phosphorylation and nuclear translocation of PKM2 promotes the Warburg effect. *Nat. Cell Biol.* **14**, 1295-1304. doi:10.1038/ncb2629
- Yang, C., Ko, B., Hensley, C. T., Jiang, L., Wasti, A. T., Kim, J., Sudderth, J., Calvaruso, M. A., Lumata, L., Mitsche, M. et al. (2014). Glutamine oxidation maintains the TCA cycle and cell survival during impaired mitochondrial pyruvate transport. *Mol. Cell* **56**, 414-424. doi:10.1016/j.molcel.2014.09.025
- Zhang, H., Bagherie-Lachidan, M., Badouel, C., Enderle, L., Peidis, P., Bremner, R., Kuure, S., Jain, S. and McNeill, H. (2019). FAT4 fine-tunes kidney development by regulating RET signaling. *Dev. Cell* **48**, 780-792.e4. doi:10.1016/j.devcel.2019.02.004
- Zhao, T., Goh, K. J., Ng, H. H. and Vardy, L. A. (2012). A role for polyamine regulators in ESC self-renewal. *Cell Cycle* **11**, 4517-4523. doi:10.4161/cc.22772
- Zhou, H.-L., Zhang, R., Anand, P., Stomberski, C. T., Qian, Z., Hausladen, A., Wang, L., Rhee, E. P., Parikh, S. M., Karumanchi, S. A. et al. (2019). Metabolic reprogramming by the S-nitroso-CoA reductase system protects against kidney injury. *Nature* **565**, 96-100. doi:10.1038/s41586-018-0749-z